Precision Rectification of SPOT Imagery Using the Direct Linear Transformation Model

Yasser El-Manadili and Kurt Novak

Abstract

A simple rigorous method for the geometric processing of SPOT images is formulated and evaluated. This method is based on the Direct Linear Transformation (DLT) model, which is employed after correcting the image coordinates for systematic distortions caused by Earth rotation and cell size variations due to off-nadir viewing. Corrections for other types of systematic errors are considered through the adjustment.

Several experiments are presented using synthetic and real data to evaluate the new method. Simulated data are generated from a general model that imitates the SPOT orbit using the Eulerian parameters, satellite deviations, and velocity vectors, as well as sensor attitude angles as functions of time. The results show that sub-pixel accuracy can be achieved with as few as six control points, if control point errors are kept small. Different parameters that influence the accuracy of the resulting ground coordinates are studied; they include the number and quality of ground control points, image coordinate errors, and base-to-height ratio.

Introduction

During the past decade, spatial topographic mapping from space gained popularity. Satellite photogrammetry has the potential of becoming the favorite method for fast and systematic map production on a regional and global basis. Satellite images are near orthographic projections of the Earth's surface, are already separated in color, and are available in a digital form that can be easily incorporated into geographic information systems. The SPOT system is able to acquire high resolution stereo imagery of almost all of the Earth's surface.

A SPOT scene is built up by combining a sequence of scan lines which are recorded over a 9-second period, resulting in a 6000- by 6000-pixel image for panchromatic mode, and a 3000- by 3000-pixel image for the multispectral mode. The orientation of the scene as well as the positions of the frame center and corners can be determined using the well known orbit characteristics recorded by the satellite's attitude and altitude control systems. The predicted ephemeris is available from SPOT Image Corporation for each scene. Deviations of the exposure centers from their nominal positions, together with the effects of the changes of the attitude angels, introduce errors of about 500 metres between the true and the calculated ground positions of the scene (SPOT User's Handbook, 1988).

SPOT scenes must be geometrically rectified in order to reach accuracies that are suitable for the production of 1:100,000- or 1:50,000-scale topographic maps. A commonly used modeling technique is to apply a low-order polynomial to correct distortions of the scene relative to the map. The advantages of this approach are the simple implementation and no need for the satellite orbit and sensor calibration parameters. However, its disadvantages are the necessity of a large number of well distributed ground control points, the lack of a physical interpretation of the model, and the dependency of the chosen polynomial on image and terrain characteristics, because different polynomials are required for each image. Another modeling approach combines *a priori* orbit data with ground control points in a simultaneous adjustment. Better results can be achieved and the number of ground control points is reduced. This model is general and suitable for any SPOT image.

Numerous articles have been published on various techniques of modeling the SPOT imaging system (Dowman, 1985; Gugan, 1987; Gugan and Dowman, 1988; Konceny and Lohmann, 1987; Mikhail, 1988; Nagy, 1988; Kratky, 1989; Westin, 1990; Makki, 1991; Mikhail and Paderes, 1991). In this paper a new method will be developed to precisely rectify SPOT imagery. The image coordinates are first geometrically corrected for the effects of Earth rotation and cell-size variations due to oblique viewing angles. Other systematic errors are considered through the least-squares adjustment procedure. The general collinearity equations for push-broom scanners are modified to the Direct Linear Transformation (DLT) equations. A least-squares adjustment solves these equations using a minimum of six ground control points to determine the 11 orientation parameters of a scene. Ground point intersection is implemented to calculate independently the ground coordinates of object points. The model is tested using synthetic and real data. The results show the potential of using the new technique for rectifying SPOT imagery.

In the following, we first define image and ground coordinate systems, and then derive the linear mathematical model. Equations used for the geometric corrections of the systematic errors are formulated next. Then we describe the implementation of the model and the performed tests using simulated and real data. Finally, the accuracy of the computed ground coordinates is evaluated.

Definition of Image and Ground Coordinate Systems

The image coordinate system defined in a SPOT scene is two-dimensional. It has its origin at the left upper corner of the image, the u-axis is in the direction of increasing row numbers, and the v-axis is perpendicular to it (see Figure 1). The pixel coordinates (u,v) can be converted to metric image coordinates (x,y) by

Department of Geodetic Science and Surveying, The Ohio State University, Columbus, OH 43210-1247.

Y. El-Manadili is presently with the Faculty of Engineering, Cairo University, Egypt.

K. Novak is presently with Transmap Corporation, 1275 Kinnear Road, Suite 109, Columbus, OH 43212-1155.

Photogrammetric Engineering & Remote Sensing, Vol. 62, No. 1, January 1996, pp. 67–72.

0099-1112/96/6201-67$3.00/0

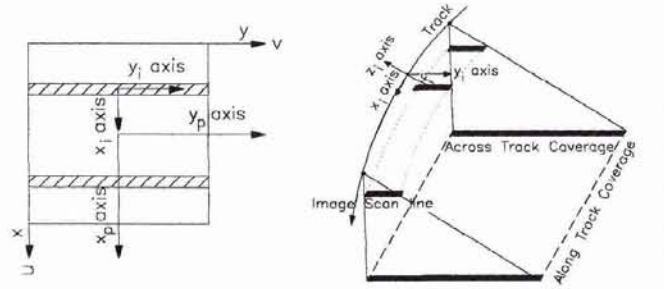

Figure 1. Definition of image coordinate systems and the SPOT sensor geometry.

$$x = u\,d \qquad y = v\,d \tag{1}$$

where u is the image row number, v is the image column number, and d is the image pixel resolution (13 μm for SPOT).

The ground coordinate system is a Shifted Geocentric Ground Coordinate System (SGCGCS). The Geocentric Ground Coordinate System (GCGCS) has its origin at the center of gravity of the Earth, its X_G and Y_G axes are in the equatorial plane, the X_G axis is directed towards the Greenwich meridian, the Z_G axis points towards the north pole, and the three axes constitute a right-handed system. Ground control coordinates are measured from large-scale topographic maps or by using the Global Positioning System (GPS). They are transformed to the GCGCS knowing the characteristics of the reference ellipsoid (GRS80) and then are shifted to the center of the area covered by the scenes (see Figure 2) as follows:

$$\mathbf{X}_{Gs} = \mathbf{X}_G - \mathbf{D}_F \tag{2}$$

where $\mathbf{X}_{Gs}$ are ground coordinates in the SGCGCS, $\mathbf{X}_G$ are ground coordinates in the GCGCS, and $\mathbf{D}_F$ are GCGCS coordinates of the center of the ground area.

Derivation of the Mathematical Model

The SPOT sensor is a moving-perspective-center imaging system. Different scan-line coordinate systems can be defined at different time intervals (ΔT) with respect to its frame center. On the other hand, a regular frame photograph has only a single image coordinate system defined at the time of exposure. The transformation between this system and the ground is described by the regular collinearity equations. For push-broom systems, each scan line has its own central perspective relationship with the ground. Its parameters are time dependent and highly correlated between neighboring scan lines.

The metric image coordinates of any point can be expressed as functions of the image row number (u), the image column number (v), the row and column numbers of the frame center (u_f,v_f), and the image pixel resolution (d) (see Figure 1) as follows:

Scan-line coordinates (Makki, 1991):

$$\begin{aligned} x_i &= (u - \text{int}(u) - 0.5)\,d \\ y_i &= (v - v_f)\,d \\ z_i &= -f_i = -1.082 \text{ m} \end{aligned} \tag{3}$$

Frame coordinates:

$$\begin{aligned} x_p &= (u - u_f)\,d \\ y_p &= (v - v_f)\,d \\ z_p &= -f_p = -1.082 \text{ m} \end{aligned} \tag{4}$$

where x_p, y_p are the metric image coordinates with respect to the frame coordinate system; x_i, y_i are the metric image coordinates with respect to the scan-line coordinate system; and f_p, f_i are the focal lengths of the two systems (int means truncated).

In order to apply the regular collinearity equations to the image coordinates of a point, they must first be transformed to the frame coordinate system by adding certain corrections to their values. Additionally, one must correct frame coordinates for the effects of satellite deviations from nominal positions, perturbations in satellite velocity vectors, and rate of changes of the sensor attitude angles. The corrections to the image coordinates (δ_x,δ_y) can be written as follows:

$$\delta_x = c_1 + c_2\,x_i + c_3\,\Delta T \tag{5}$$

$$\delta_y = c_4 + c_5\,y_i + c_6\,\Delta T \tag{6}$$

where c_1, c_2, ..., c_8, and c_6 are constant values for the whole scene; ΔT is the time with respect to the frame center ($u - u_f$)S_t; and S_t is the sampling time = 0.0015 second per scan line.

Geometric corrections of systematic distortions caused by Earth rotation and off-nadir viewing are applied to the image row and column numbers before the adjustment, in order to reduce the effects of scan-line shifts and relief displacements, respectively.

Equations 5 and 6 can now be reduced as follows:

$$\begin{aligned} \delta_x &= c_1 + c_2\,x_i + c_3\,\Delta T \\ &= c_1 + c_2\,(u - \text{int}(u) - 0.5)d + c_3\,(u - u_f)\,S_t = c_7 + c_8\,u\,d \end{aligned} \tag{7}$$

$$\begin{aligned} \delta_y &= c_4 + c_5\,y_i + c_6\,\Delta T \\ &= c_4 + c_5\,(v - v_f)\,d + c_6\,(u - u_f)\,S_t = c_9 + c_{10}\,v\,d + c_{11}\,u\,d \end{aligned} \tag{8}$$

Thus, the corrected image coordinates (x', y') can be written as

$$\begin{aligned} x_p' &= x_p + \delta_x \\ &= (u - u_f)\,d + c_7 + c_8\,u\,d = [c_7 - u_f\,d] + [c_8 + 1]\,u\,d \\ &= d_1 + d_2\,(u\,d) = d_1 + d_2\,x \end{aligned} \tag{9}$$

$$\begin{aligned} y_p' &= y_p + \delta_y \\ &= (v - v_f)\,d + c_9 + c_{10}\,v\,d + c_{11}\,u\,d \\ &= [c_9 - v_f d] + [c_{10} + 1]\,v\,d + c_{11}\,u\,d \\ &= d_3 + d_4\,(v\,d) + d_5\,(u\,d) = d_3 + d_4\,y + d_5\,x \end{aligned} \tag{10}$$

In matrix form, we get:

$$\begin{bmatrix} x_p' \\ y_p' \\ -f \end{bmatrix} = \begin{bmatrix} d_2 & 0 & d_1 \\ d_5 & d_4 & d_3 \\ 0 & 0 & -f \end{bmatrix} \cdot \begin{bmatrix} x \\ y \\ 1 \end{bmatrix} \tag{11}$$

Equation 11 establishes a direct relationship between the measured image coordinates (x,y) relative to the left upper

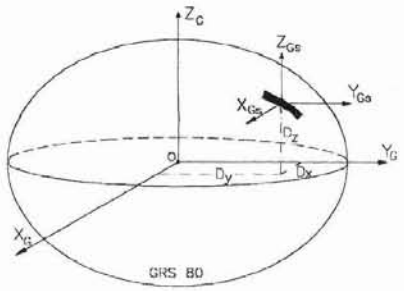

Figure 2. Definition of the Geocentric and Shifted Geocentric Ground Coordinate Systems.

corner of the image, and corrected frame coordinates (x'_p, y'_p) that can be used in the regular collinearity equations. Thus, this relationship transforms pixel coordinates of a push-broom image into corrected central perspective coordinates of a frame image.

Next, the collinearity equations are combined with the corrected image coordinates as follows:

$$\begin{bmatrix} d_2 & 0 & d_1 \\ d_5 & d_4 & d_3 \\ 0 & 0 & -f \end{bmatrix} \cdot \begin{bmatrix} x \\ y \\ 1 \end{bmatrix} = S \cdot \mathbf{M} \cdot \left(\begin{bmatrix} X_{Gs} \\ Y_{Gs} \\ Z_{Gs} \end{bmatrix} - \begin{bmatrix} X_C \\ Y_C \\ Z_C \end{bmatrix} \right) \quad (12)$$

Simplified in matrix form, this transformation becomes

$$\mathbf{M}_i \cdot \mathbf{x}_i = S \cdot \mathbf{M} \cdot (\mathbf{X}_{Gs} - \mathbf{X}_C) \quad (13)$$

where

$\mathbf{x}_i$ = image coordinate vector,
$\mathbf{X}_{Gs}$ = ground control point vector,
S = scale factor,
$\mathbf{M}$ = rotation matrix between the SGCGCS and the Corrected Frame Coordinate System (CFCS),
$\mathbf{X}_C$ = coordinates of the exposure center of the CFCS, and
$\mathbf{M}_i$ = matrix of the corrections and transformation parameters between the original image coordinate system and the CFCS, as defined in Equation (11):

that is,

$$\mathbf{X}_{Gs} - \mathbf{X}_C = \begin{bmatrix} X_{Gs} \\ Y_{Gs} \\ Z_{Gs} \end{bmatrix} - \begin{bmatrix} X_C \\ Y_C \\ Z_C \end{bmatrix} = \begin{bmatrix} 1 & 0 & 0 & -X_C \\ 0 & 1 & 0 & -Y_C \\ 0 & 0 & 1 & -Z_C \end{bmatrix} \cdot \begin{bmatrix} X_{Gs} \\ Y_{Gs} \\ Z_{Gs} \\ 1 \end{bmatrix} \quad (14)$$

Therefore, the image coordinates can be expressed as functions of the ground coordinates as follows:

$$\begin{aligned} \mathbf{x}_i &= S \cdot \mathbf{M}_i^{-1} \cdot \mathbf{M} \cdot (\mathbf{X}_{gs} - \mathbf{X}_C) \\ &= (S/-d_2 d_4 f) \cdot \begin{bmatrix} -d_4 f & 0 & -d_1 d_4 \\ d_5 f & -d_2 f & -d_2 d_3 + d_1 d_5 \\ 0 & 0 & d_2 d_4 \end{bmatrix} \\ &\quad \cdot \begin{bmatrix} m_{11} & m_{12} & m_{13} \\ m_{21} & m_{22} & m_{23} \\ m_{31} & m_{32} & m_{33} \end{bmatrix} \cdot \begin{bmatrix} 1 & 0 & 0 & -X_c \\ 0 & 1 & 0 & -Y_c \\ 0 & 0 & 1 & -Z_c \end{bmatrix} \cdot \begin{bmatrix} X_{Gs} \\ Y_{Gs} \\ Z_{Gs} \\ 1 \end{bmatrix} \\ &= (S/d_2 d_4 f) \cdot \begin{bmatrix} a_{11} & a_{12} & a_{13} & a_{14} \\ a_{21} & a_{22} & a_{23} & a_{24} \\ a_{31} & a_{32} & a_{33} & a_{34} \end{bmatrix} \cdot \begin{bmatrix} X_{Gs} \\ Y_{Gs} \\ Z_{Gs} \\ 1 \end{bmatrix} \end{aligned} \quad (15)$$

where

$$\begin{aligned} a_{11} &= d_4 f m_{11} + d_4 d_1 m_{31}, \; a_{12} = d_4 f m_{12} + d_4 d_1 m_{32}, \\ a_{13} &= d_4 f m_{13} + d_4 d_1 m_{33}, \; a_{14} = -d_4 f A_1 + d_4 d_1 A_3, \\ a_{21} &= -d_5 f m_{11} + d_2 f m_{21} + d_2 d_3 m_{31} - d_1 d_5 m_{31}, \\ a_{22} &= -d_5 f m_{12} + d_2 f m_{22} + d_2 d_3 m_{32} - d_1 d_5 m_{32}, \\ a_{23} &= -d_5 f m_{13} + d_2 f m_{23} + d_2 d_3 m_{33} - d_1 d_5 m_{33}, \\ a_{24} &= d_5 f A_1 - d_2 f A_2 - d_2 d_3 A_3 + d_1 d_5 A_3, \\ a_{31} &= -d_2 d_4 m_{31}, \; a_{32} = -d_2 d_4 m_{32}, \\ a_{33} &= -d_2 d_4 m_{33}, \; a_{34} = d_2 d_4 A_3, \\ A_1 &= m_{11} X_C + m_{12} Y_C + m_{13} Z_C, \\ A_2 &= m_{21} X_C + m_{22} Y_C + m_{23} Z_C, \\ A_3 &= m_{31} X_C + m_{32} Y_C + m_{33} Z_C \end{aligned}$$

After some modifications, Equation 15 can be written as Equations 16 and 17, which are identical to the conventional Direct Linear Transformation model (Abed El-Aziz and Karara 1971): i.e.,

$$x = \frac{L_1 X_{Gs} + L_2 Y_{Gs} + L_3 Z_{Gs} + L_4}{L_9 X_{Gs} + L_{10} Y_{Gs} + L_{11} Z_{Gs} + 1} \quad (16)$$

$$y = \frac{L_5 X_{Gs} + L_6 Y_{Gs} + L_7 Z_{Gs} + L_8}{L_9 X_{Gs} + L_{10} Y_{Gs} + L_{11} Z_{Gs} + 1} \quad (17)$$

Equations 16 and 17 can be rearranged as Equation 18: i.e.,

$$\begin{aligned} F_x &= x - L_1 X_{Gs} - L_2 Y_{Gs} - L_3 Z_{Gs} - L_4 + L_9 x X_{Gs} \\ &\quad + L_{10} x Y_{Gs} + L_{11} x Z_{Gs} = 0 \\ F_y &= y - L_5 X_{Gs} - L_6 Y_{Gs} - L_7 Z_{Gs} - L_8 + L_9 y X_{Gs} \\ &\quad + L_{10} y Y_{Gs} + L_{11} y Z_{Gs} = 0 \end{aligned} \quad (18)$$

where L_1, L_2, ..., L_{10}, and L_{11} are the eleven linear orientation parameters between two-dimensional image space and three-dimensional object space. They are functions of the five correction and transformation and transformation parameters $(d_1, ..., d_5)$ and the six exterior orientation parameters of the CFCS:

$$\begin{aligned} &L_1 = -a_{11}/a_{34}, \; L_2 = -a_{12}/a_{34}, \; L_3 = -a_{13}/a_{34}, \; L_4 = -a_{14}/a_{34}, \\ &L_5 = -a_{21}/a_{34}, \; L_6 = -a_{22}/a_{34}, \; L_7 = -a_{23}/a_{34}, \; L_8 = -a_{24}/a_{34}, \\ &L_9 = a_{31}/a_{34}, \; L_{10} = a_{32}/a_{34}, \; L_{11} = a_{33}/a_{34}. \end{aligned}$$

Geometric Corrections

The image coordinates (u,v) have to be corrected for systematic errors caused by the rotation of the Earth and off-nadir viewing before the above model can be practically applied. The analytical formulas are explained below.

Earth Rotation

The Earth rotates around its axis with a mean velocity (V_e) of 0.00007272205 rad/sec. This introduces errors in the image coordinates in the row and column directions. The distortions of the scene depend on many factors, such as orbit inclination (i), incidence angle of the scene (Γ), and latitude of the frame center (Φ). They can be corrected using the following equations:

$$\begin{aligned} D_u &= V_e R_n \cos(\Phi_o) \sin(\gamma) (S_t u)/d_g \\ D_v &= V_e R_n \cos(\Phi_o) \cos(\gamma) (S_t u)/d_g \end{aligned} \quad (19)$$

where

D_u, D_v = corrections to the row and column numbers, respectively;
Φ_o = geocentric latitude of the ground point = $\tan^{-1}[(b_e^2/a_e^2)\tan(\Phi)]$;
R_n = $b_e/(1 - (\cos(\Phi_o))^2/149)^{0.5}$;
a_e, b_e = semi-major and semi-minor axes of the GRS 80 ellipsoid;
γ = orientation angle of the scene, which is the angle made by the meridian with the perpendicular to the center line of the scene;
$\sin(\gamma)$ = $[\sin(\Phi_o)\sin(\Gamma - \omega) - \cos(i)]/[\cos(\Phi_o)\cos(\Gamma - \omega)]$; and
d_g = ground pixel resolution, which has a nominal value of 10 m.

Off-Nadir Viewing

SPOT off-nadir viewing causes cell-size variations in the direction of increasing column numbers. Knowing the off-nadir viewing angle of the scene, column numbers of any image point can be corrected using the following equations (see Figure 3):

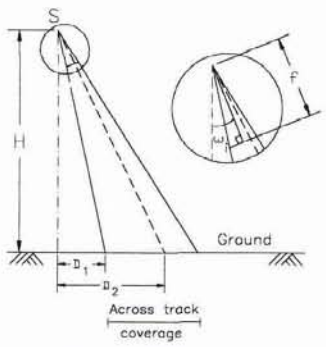

Figure 3. Correction of image coordinates for off-nadir viewing.

$$a = \tan^{-1}(d/f) \quad (20)$$

$$D_1 = H \tan(w_i - v_f a) \quad (21)$$

$$D_2 = H \tan(w_i - v_f a + v\, a) \quad (22)$$

where d is the image pixel resolution; a is the angle subtended by one image pixel at the frame center; H is the satellite height above the ellipsoid; w_i is the off-nadir viewing angle of the scene; and D_1, D_2 are the ground distances from the nadir point to the left hand corner of the scan line and the image point, respectively.

Measured and corrected ground distances in the v direction (d_m, d_c) are determined as follows:

$$d_m = v\, d_g, \qquad d_c = D_2 - D_1 \quad (23)$$

Thus, the corrected column number (V_c) is given by

$$V_c = v\,(d_c/d_m) \quad (24)$$

Implementation

The total restitution process is shown in the flow chart (Figure 4). The image coordinates as well as the coordinates of the ground control points (latitudes, longitudes, and heights above the ellipsoid) serve as input to the program, which is written with MATLAB on a Sun workstation, but could be easily implemented on any inexpensive 486 microcomputer. The data to be extracted from the leader file of the SPOT

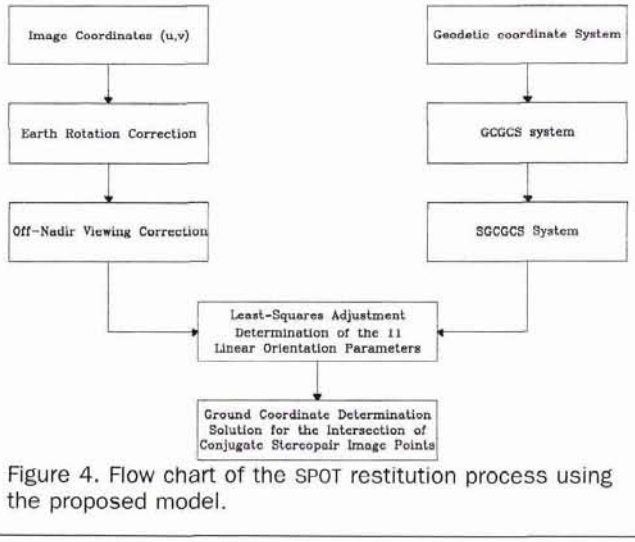

Figure 4. Flow chart of the SPOT restitution process using the proposed model.

TABLE 1. SPECIFICATIONS OF TERRAINS AND SPOT STEREO-PAIRS USED FOR SIMULATION

Experiment	Left Image roll pitch yaw	Right Image roll pitch yaw	Terrains	No. of GCP.	*B*-to-*H* ratio
A (1,2,3)	10 −0.3 1.0	−10 0.5 −1.0	Hilly	6,9,12	0.4
B (1,2,3)	20 −0.3 1.0	−20 0.5 −1.0	Hilly	6,9,12	0.8
C (1,2,3)	27 −0.3 1.0	−27 0.5 −1.0	Hilly	6,9,12	1.1
D (1,2,3)	20 0.0 0.0	−20 0.0 0.0	Flat	6,9,12	0.8

stereo-pair are the off-nadir viewing angles, which can be easily determined from the mirror step numbers or the incidence angles of the left and the right images, the orientation angles of the scenes, as well as the latitude and longitude of the ground nadir point. The adjustment yields the following parameters:

- The eleven linear orientation parameters (L_1, ..., L_{11}) of the left and right images,
- Three-dimensional coordinates (X_G, Y_G, Z_G) of tie and check points, and
- Variances and covariances of the unknowns.

Rectification Results

Many experiments were conducted using synthetic data in order to evaluate the new method. The data were generated from a strict analytical model that relates the image to the ground using the Eulerian orbital parameters (longitude of ascending node, orbit inclination, true anomaly, orbit semi-major axis, and orbit eccentricity). The true anomaly is considered to be variable with time together with the distance from the sensor exposure center to the center of gravity of the Earth. The general model transformation equations contain the effect of the attitude angles, their rates of change with respect to time, satellite deviations from nominal positions as functions of the perturbations in the satellite velocity and acceleration vectors.

Different sets of check point distributions were simulated, including completely flat terrains and hilly terrains with elevations varying up to 500 metres. The number of check points ranged from 25 to 50 for different tests. The RMS errors in the X_G, Y_G, and Z_G directions and their standard deviations were calculated by comparing triangulation results with known check point coordinates. Then, the error components in the Northing, Easting, and Height directions were also obtained. The results show that the errors do not exceed one pixel for any kind of terrain with elevation differences less than or equal to 500 metres and a base-to-height ratio equal to 0.8 . Tables 1 and 2 show samples of the results for some of the test cases.

In similar tests, the effects of satellite deviations from their nominal positions and rates of changes of the attitude angles were studied. Different values for the perturbations in the satellite velocity and acceleration vectors were used. Variations of the attitude angles were taken from the leader files of some real SPOT stereo-pairs. The results show that the RMS errors of the ground coordinates are nearly the same as in the previous tests.

The developed method was also tested using real data. A SPOT panchromatic stereo-pair taken over Nevada was used (see Figure 5). The off-nadir viewing angles are 7.36° and 10.04° to the east and the west, respectively. The area covered by the scenes extends from latitudes 37°3'30.5"N to 37°37'47.7"N and longitudes 116°3'37"W to 116°32'36.6"W. The mean ground elevation is 548 metres above the ellipsoid, and height differences vary up to 310 metres. The area is covered by 36 USGS 1:24,000-scale quad sheets. On these maps 12 well defined points were digitized with a mean accuracy of 10 metres. The marking of the positions of these

TABLE 2. GROUND COORDINATE RMS ERRORS DERIVED AT THE 50 CHECK POINTS FOR SIX OF THE TEST CASES

Case number	X_G	Y_G	Z_G
C-1	4.76	3.19	3.51
C-2	4.78	3.68	3.59
C-3	5.14	3.15	3.61
D-1	4.54	3.16	2.82
D-2	4.52	3.18	2.82
D-3	4.54	3.21	2.85

C-1 refers to experiment C using six control points, C-2 uses nine control points, etc.

points in the scenes was made by manual pixel pointing, using the cursor on a computer screen with an accuracy of 1 pixel. Six control points were used in the adjustment. The RMS errors were calculated for the control and check points, respectively. The results are presented in Table 3.

Model Analysis and Evaluation

A complete simulation study was conducted in order to examine each factor that may affect the ground coordinate accuracy, such as the number and quality of ground control points, the measurement accuracy of the image coordinates, and the base-to-height ratio. Different numbers of control points (6 to 15 points) were used with error free image coordinates (Table 2). In other tests, random errors were added to the image and ground control coordinates. Random errors have normal distributions with standard deviation values ranging from 1 to 4 pixels for the image coordinates and 0.1 to 5 metres for the ground coordinates of the control points. Finally, the effect of the base-to-height ratio was examined and samples of the results were graphically represented.

Figure 6 shows the RMS errors in the simulated data sets at the 50 check points for the flat and hilly terrains, when using different numbers of ground control points. Ground coordinate errors are increasing with an increase of the elevation differences between the terrain points. More control points than the minimum (six control points) do not improve the accuracy, when image and ground control coordinates are precisely measured.

TABLE 3. GROUND COORDINATE ERRORS DERIVED FOR THE SPOT SCENE SHOWN IN FIGURE 5

S	X_G	Y_G	Z_G
Control points	2.38	3.24	2.70
Check points	13.43	18.91	19.74

S: Standard deviation at the six control points computed from adjustment; and mean errors at the 12 check points.

Figure 7 displays the effects of the measurement accuracy of the image coordinates on the ground coordinates of the check points. The ground RMS error at any image coordinate measurement accuracy is nearly equal to the ground error at one pixel coordinate accuracy times the measurement accuracy in pixels. The accuracy is not improved by increasing the number of ground control points.

Figure 8 shows the effect of the measurement accuracy of the coordinates of the ground control points. The relationship between ground coordinate random errors and the resulting ground RMS errors are basically linear for all cases, and for any number of ground control points. Adding more control points reduce the ground RMS errors. It may be decreased by 3 to 5 metres when increasing the number of the control points from 6 to 9 and 12, respectively.

The distribution of the control points is very important, and the resulting positional accuracy is affected by a weak distribution. The effects of the attitude rates of changes and the small perturbations in the satellite velocity and acceleration vectors are absorbed by the adjustment.

Figure 9 represents the relationship between the base-to-height ratio and the resulting ground coordinate accuracy. As expected, the accuracy is improved by increasing the base-to-height ratio, which results in a better intersection geometry.

Conclusions

A new direct linear model for orienting SPOT scenes was presented in this paper. The results of simulations and real scenes show the potential of using the new method for rectifying SPOT imagery. Accuracies better than a pixel can be achieved with a small number of ground control points, if control and image point errors are kept small. The whole procedure takes a very short time (less than 3 seconds). After determining the linear orientation parameters, image and ground coordinates can be determined using the image and ground point intersection algorithms in a very simple manner.

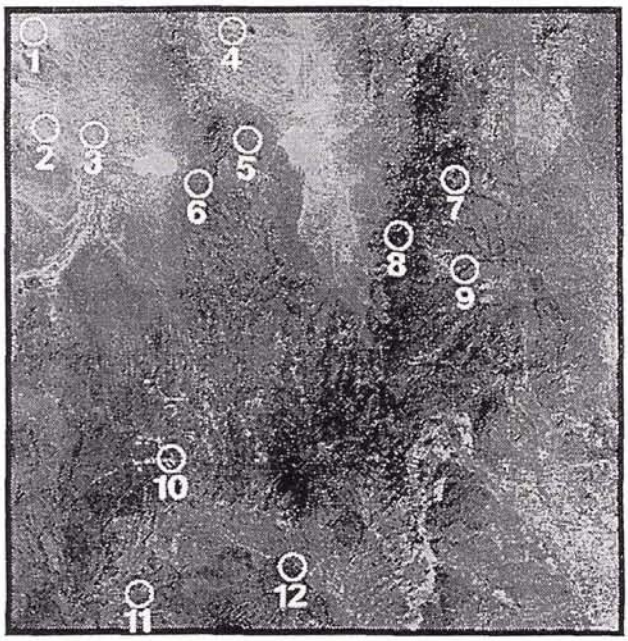

Figure 5. A SPOT panchromatic stereo-pair, taken over Nevada.

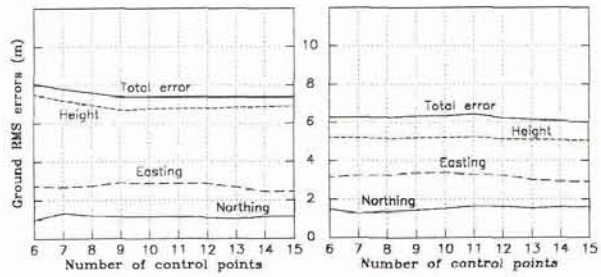

Figure 6. Ground RMS errors at the check points, using different numbers of ground control points.

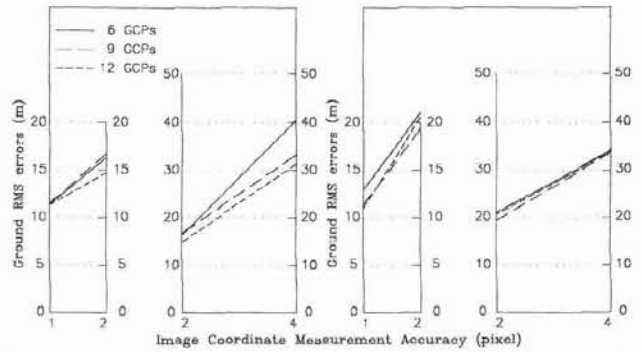

Figure 7. Ground RMS errors at the check points, dependent upon the image coordinate measurement accuracy.

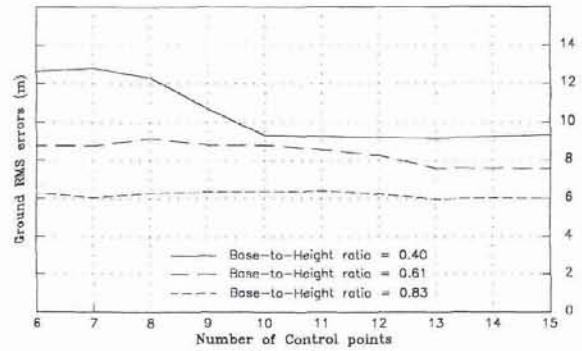

Figure 9. Ground RMS errors at the check points, dependent upon the base-to-height ratio.

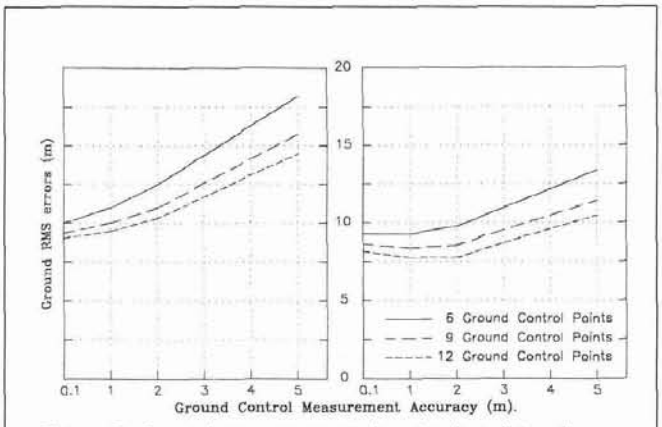

Figure 8. Ground RMS errors at the check points, dependent upon the ground control measurement accuracy.

Acknowledgments

Acknowledgment is made to the Byrd Polar Research Center and the Center for Mapping, The Ohio State University, which provided the facilities and equipment to finish this research. Thanks are also extended to all the staff of the Surveying Department, Faculty of Engineering, Cairo University, Egypt, especially to Prof. Abed El-Lattif Sabbah, Prof. Shawki El-Ghazali, Prof. Youssef Abed El-Aziz, and Dr. Ashraf Nasr Sayed for their cooperation.

References

Abed El-Aziz, Y.A., and H.M. Karara, 1971. Direct Linear Transformation from Comparator Coordinates into Object Space Coordinates in Close-Range Photogrammetry, *Proceedings of the ASP/UI Symposium on Close-Range Photogrammetry*, Urbana, pp. 420–475.

Dowman, I.J., 1985. Images from Space: Future for Satellite Photogrammetry, *Photogrammetric Record*, 11(65):507–513.

Gugan, D.J., 1987. Practical Aspects of Topographic Mapping from SPOT Imagery, *Photogrammetric Record*, 12(69):349–355.

Gugan, D.J., and I.J. Dowman, 1988. Topographic Mapping from SPOT Imagery, *Photogrammetric Engineering & Remote Sensing*, 54(10):1409–1414.

Konceny, G., and P. Lohmann, 1987. Evaluation of SPOT Imagery on Analytical Photogrammetric Instruments, *Photogrammetric Engineering & Remote Sensing*, 53(9):1223–1230.

Kratky, V., 1989. Rigorous Photogrammetric Processing of SPOT Images at CCM Canada, *ISPRS Journal of Photogrammetry and Remote Sensing*, 44:53–71.

Makki, S.A., 1991. *Photogrammetric Reduction and Analysis of Real and Simulated SPOT Imageries*, Ph.D. Dissertation, School of Civil Engineering, Purdue University, West Lafayette, Indiana.

Mikhail, E.M., 1988. *Photogrammetric Modeling and Reduction of SPOT Stereo Images*, Technical Report, Purdue University, West Lafayette, Indiana.

Mikhail, E.M., and F.C. Paderes, 1991. *Photogrammetric Modeling and Reduction of SPOT Stereo Images (Phase II)*, Final Technical Report for USGS, School of Civil Engineering, Purdue University, West Lafayette, Indiana.

Nagy, T.M., 1988. "Large Area Triangulation with SPOT Imagery", paper presented at the Annual Convention ASPRS, St. Louis, Missouri.

Paderes, F.C., and E.M. Mikhail, 1988. Batch and On-line Evaluation of SPOT Stereo Imagery, *ACSM-ASPRS Annual Convention*, 3: 31–40.

SPOT Image Corporation, 1989a. *SPOT User's Handbook—Reference Manual*, Volume 1, Center Spatial de Toulouse.

———, 1989b. *SPOT User's Handbook—SPOT Handbook*, Volume 2, Center Spatial de Toulouse.

Westin, T., 1990. Precision Rectification of SPOT Imagery, *Photogrammetric Engineering & Remote Sensing*, 56(2):247–253.

(Received 2 September 1993; revised and accepted 31 October 1994)